Applied Magnetic Resonance (2021) 52:337–348
https://doi.org/10.1007/s00723-021-01310-9

Applied
Magnetic Resonance

REVIEW

Spin Dynamics in Quantum Sine-Gordon Spin Chains: High-Field ESR Studies

Sergei Zvyagin[1]

Received: 28 August 2020 / Revised: 29 December 2020 / Accepted: 6 January 2021 /
Published online: 24 February 2021

Abstract

A spin-1/2 Heisenberg antiferromagnetic chain is one of the most important paradigmatic models in quantum magnetism. Its ground state is a spin singlet, while the excitation spectrum is formed by gapless fractional excitations, spinons. The presence of alternating g-tensors and/or the staggered Dzyaloshinskii-Moriya interaction results in opening the energy gap $\Delta \propto H^{2/3}$, once the magnetic field H is applied. A fairly good understanding of this phenomenon was achieved in the framework of the sine-Gordon quantum-field theory, taking into account the effective transverse staggered field induced by the applied uniform field. The theory predicts solitons and antisolitons as elementary excitations, as well as their bound states, breathers. Here, I review recent high-field electron spin resonance spectroscopy studies of such systems, focusing on peculiarities of their spin dynamics in the sine-Gordon regime and beyond.

Low-dimensional (low-D) quantum magnets attract a lot of attention serving as an excellent playground for testing numerous theoretical concepts of condensed-matter physics and quantum magnetism [1]. Among others, a spin-1/2 Heisenberg antiferromagnetic (AF) chain with the uniform nearest-neighbor exchange coupling is one of the most important model systems, whose magnetic properties are well understood. Its ground state is a non-magnetic spin singlet, and the spin dynamics is determined by a gapless two-particle continuum of fractional spin-1/2 excitations, spinons. The energies of the upper and lower boundaries of the continuum are given as

$$\varepsilon_u(q) = \frac{\pi}{2} J |\sin(q/2)|, \tag{1}$$

and

✉ Sergei Zvyagin
s.zvyagin@hzdr.de

[1] Dresden High Magnetic Field Laboratory (HLD-EMFL), Helmholtz-Zentrum Dresden-Rossendorf, 01328 Dresden, Germany

$$\varepsilon_l(q) = \frac{\pi}{2} J |\sin(q)|, \tag{2}$$

respectively (where J is the nearest-neighbor interchange coupling and q is the wave vector) [2]. Application of the uniform magnetic field results in a substantial rearrangement of the excitation spectrum, making the soft modes incommensurate [3], but leaving the excitation continuum gapless up to the saturation field $H_{\rm sat}$.

The situation is considerably different in case of a spin-1/2 Heisenberg AF chain with the alternating g-tensor and/or staggered Dzyaloshinskii-Moriya (DM) interaction. The application of the uniform field H opens the energy gap $\Delta \propto H^{2/3}$. Such a behavior has been recently described in terms of the sine-Gordon quantum-field theory [4–6], with the effective transverse staggered field playing a key role in the gap formation. For sine-Gordon spin chains the theory predicts the presence of solitons, antisolitons, and multiple soliton-antisoliton bound states, called breathers [7, 8]. Above $H_{\rm sat}$, quantum effects are significantly suppressed and the excitation spectrum is determined by ordinary gapped magnons [9–11]. Another consequence of such an alternation is the specific temperature and field behavior of electron spin resonance (ESR) parameters (the linewidth and effective g-factor) [12, 13]. These properties are realized in Cu-benzoate [14–20], Cu-PM [21–24], $CuCl_2{\cdot}2(CH_3)_2SO$ [25, 26], Yb_4As_3 [27–30], $KCuGaF_6$ [31–34], $CuSe_2O_5$ [35], and $KCuMoO_4(OH)$ [36].

ESR spectroscopy is traditionally recognized as one of the most powerful means for probing magnetic-excitation spectra in exchange-coupled spin systems with the exceptional resolution and sensitivity. Using temperature or magnetic field as variable parameters, one can obtain valuable information on the nature of the ground and excited states, and estimate the spin Hamiltonian parameters. As radiation sources, one can use solid-state generators (such as Gunn and IMPATT diodes, VDI microwave chains, quantum-cascade lasers), as well as backward-wave oscillators, molecular-gas and free-electron lasers (see, e.g., Refs. [37–40]). Employment of high magnetic fields [up to 45 T (continuous) and c.a. 200 T (pulsed)] is of particular importance when studying the spin dynamics in magnetic systems with complex frequency-field diagrams and field-induced phase transitions. High-field ESR has proven to be one of the main spectroscopy tools to study exchange-coupled spin systems including quantum spin chains (for reviews see, e.g., Refs. [41–43])". One very important application of the high-field ESR is investigating the excitation spectrum in such systems above $H_{\rm sat}$, sometime allowing one to extract spin Hamiltonian parameters directly and with a high accuracy using the quasi-classical spin-wave-theory approach [44–46].

Here, I review experimental studies of the spin dynamics in spin-1/2 Heisenberg AF chains with alternating g-tensors and/or staggered DM interaction, performed by means of the high-field THz-range [47] ESR spectroscopy.

The Hamiltonian of a spin-1/2 AF Heisenberg chain with the alternating g-tensors and/or staggered DM interaction is given by

$$\mathcal{H} = J \sum_i \mathbf{S}_i \cdot \mathbf{S}_{i+1} + g\mu_B H \sum_i S_i^z + g\mu_B h \sum_i (-1)^i S_i^x, \tag{3}$$

where the first term corresponds to the isotropic Heisenberg interaction, the second term describes the Zeeman splitting, and the third one describes the contribution of the effective staggered field, $h \propto H$, induced by the applied uniform field H. The example of such a structure is shown in Fig. 1.

As mentioned, the presence of the effective staggered field is of particular importance here, resulting in the field-induced energy gap. The gap behavior was described in the framework of the sine-Gordon quantum-field theory [4–8]. Apart from soliton and antisoliton as elementary excitations, the theory predicts also the presence of their bound states, breathers. The frequency-field dependence of the soliton gap can be described using the equation:

$$\Delta_s = J\frac{2\Gamma(\frac{\xi}{2})v_F}{\sqrt{\pi}\Gamma(\frac{1+\xi}{2})}\left[\frac{g\mu_B H}{Jv_F}\frac{\pi\Gamma(\frac{1}{1+\xi})cA_x}{2\Gamma(\frac{\xi}{1+\xi})}\right]^{\frac{1+\xi}{2}}. \tag{4}$$

Here c is the proportionality coefficient connecting the uniform applied field H and the effective staggered field $h = cH$. The parameter $\xi = \left(2/(\pi R^2) - 1\right)^{-1}$, where R is the so-called compactification radius, and v_F has the meaning of the Fermi velocity; R and v_F known exactly as functions of $\widetilde{H} = g\mu_B H/J$ from the solutions of the Bethe ansatz equations [7]. The amplitude A_x, can be computed numerically [48]. The theory predicts $N = [1/\xi]$ breather branches B_n at a given field H, with $n = 1, \ldots N$. The breather gaps Δ_n can be calculated as:

$$\Delta_n = 2\Delta_s \sin(n\pi\xi/2), \tag{5}$$

while the soliton gap can be described using the equation:

$$E_s \simeq \sqrt{\Delta_s^2 + (Jv_F k_0)^2}. \tag{6}$$

A schematic sketch of the low-energy excitation spectrum in a sine-Gordon spin chain in a finite field is shown in Fig. 2. S and $\overline{S}$ denote solitons and antisolitons, while B_1 and B_2 correspond to the first and second breathers, respectively.

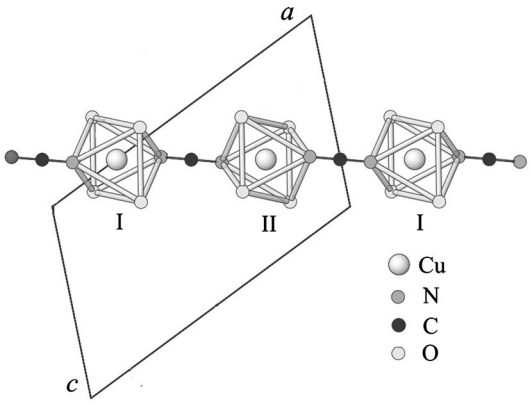

Fig. 1 A schematic view of a single chain of Cu-PM viewed along the *b*-axis. For clarity, only the ions forming octahedra along the chains, are shown. The local principal axes of each octahedron are tilted by ±29.4° from the *ac* plane, resulting in the alternating *g*-tensors. After Ref. [21]

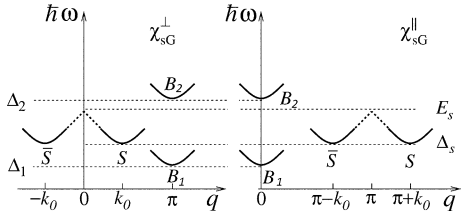

Fig. 2 A schematic sketch of the low-energy excitation spectrum in a sine-Gordon spin chain in a finite-field contributing to the transverse (left panel) and longitudinal (right panel) dynamic susceptibilities. Here, S and $\bar{S}$ denote solitons and antisolitons, while B_1 and B_2 correspond to the first and second breathers, respectively (only two lowest-energy breather states are shown). After Ref. [23]

Let me discuss experimental realizations of the sine-Gordon chain model. Cu-benzoate [chemical formula $Cu(C_6H_5COO)_2.3H_2O$] was first synthesized back in 1963 [49]. Although its low-temperature magnetic susceptibility follows the well-known Bonner-Fisher behavior for a spin-1/2 AF Heisenberg chain [50] with the exchange coupling $J/k_B = 8.6$ K [51], detailed ESR studies revealed an additional absorption below 1 K [52]. This resonance was mistakenly interpreted as a signature of AF long-range ordering. But surprisingly, later on specific heat measurements revealed the presence of the field-induced energy gap, $\Delta \propto H^{2/3}$ [14]. Such an unusual behavior does not correspond to conventional AF long-range ordering, while the anisotropic dependence of the gap strongly suggests the involvement of a anisotropy term, such as the DM interaction.

Initially, three modes of magnetic resonance were observed in Cu-benzoate using ESR with a probe in the Faraday configuration (with the radiation propagation vector parallel to the applied magnetic field, Fig. 3) [17]. Based on the frequency-field dependence of the lowest-energy mode, the energy gap as a function of magnetic

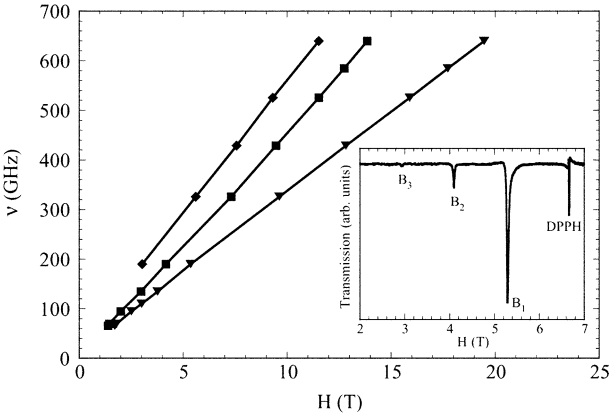

Fig. 3 Frequency-field diagram of magnetic excitations in Cu-benzoate taken at 0.5 K (measurements were performed in the Faraday configuration, $H \parallel c$). The solid lines are eye guides. An example of ESR spectrum taken at 190 GHz is given in the inset. After Ref. [17]

field was determined, revealing excellent agreement with the specific-heat data. Later on, the gap in Cu-benzoate was observed directly using an ESR probe in the Voigt configuration (with the radiation propagation vector perpendicular to the applied magnetic field; the use of the Voigt configuration is essential here, allowing the observation of ESR transitions with different selection rules) [18]. High-field ESR revealed not only the signatures of two breather excitations, B_1 and B_2 (Fig. 4), but also the inter-breather excitation X_z [20].

Cu-benzoate is in fully spin-polarized state with the saturated magnetization above $H_{sat} = 27$ T ($H \parallel c$). High magnetic fields tends to suppress quantum effects in low-D spin systems, so that above H_{sat} the excitation spectrum is supposed to be formed not by solitons and breathers, but conventional magnons. Such a crossover from the soliton-breather sine-Gordon regime to a fully spin polarized phase with magnons as elementary excitations was observed in Cu-benzoate by means of high-field ESR [20]. The crossover was studied theoretically [9–11]. In Fig. 4, the frequency-field diagram of the the low-energy ESR mode is shown together with results of the Density Matrix Renormalization Group (DMRG) calculations [10], revealing qualitatively good agreement. The peculiarities of the field-induced crossover in sine-Gordon spin chains are discussed below.

For the relevant frequency-field range, for spin-1/2 AF chains with the alternating g-tensors and staggered DM interaction the theory predicts the presence of one solitons and three soliton-antisoliton bound state excitations, breathers [7, 8]. Cu-PM [chemical formula $[PM\text{-}Cu(NO_3)_2 \cdot (H_2O)_2]_n$ (PM = pyrimidine)] has relatively strong intrachain exchange coupling, $J/k_B = 36$ K [21], allowing one to study physics of sine-Gordon spin chains at temperatures down to 1.5 K, using a conventional ^{4}He setup. The frequency-field phase diagram of magnetic excitations in Cu-PM for $H \parallel c''$ (where c'' is the axis characterized by the maximal value of the staggered magnetization) in magnetic fields up to 25 T is shown in Fig. 5. Based on the comparison with the theory, modes $B1$, $B2$, and $B3$ were identified as breather modes, while the mode S corresponds to a single-soliton excitation [23]. Thus, for the first time the complete set of the sine-Gordon

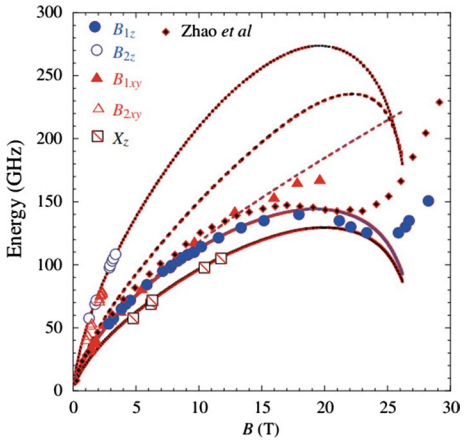

Fig. 4 Frequency-field diagrams of the breather modes B_1 and B_2 in Cu-benzoate ($H \parallel c$; x, y, z correspond to different excitation components). Mode X_z corresponds to a transition between B_{1z} and B_{2z}. The diamonds show the result of the DMRG calculations for the breather-magnon crossover around $H_{sat} = 27$ T [10], while the lines correspond to results of the sine-Gordon quantum-field theory calculations [7, 8]. After Ref. [20]

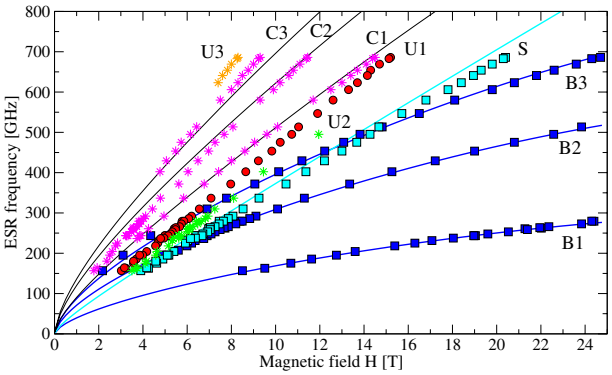

Fig. 5 Frequency-field diagram of magnetic excitations in Cu-PM in magnetic fields up to 25 T (1.6 K, $H \parallel c''$). Symbols denote the experimental results ($B1 - B3, S$ correspond to three breathers and soliton modes, respectively), while lines correspond to contributions from specific excitations as predicted by the sine-Gordon theory [7, 8]. After Ref. [23]

solutions for a $S = 1/2$ AF chain with the staggered g-tensors and DM interaction was revealed. It was explicitly shown that the field-induced gap is determined by the first breather (with the lowest excitation energy). Later on, soliton and three breathers were observed in another sine-Gordon chain systems, $KCuGaF_6$ [32].

ESR revealed significant changes in the gap behavior in Cu-PM at high fields (Fig. 6). This is in agreement with results of numerical simulations [9, 10], where a non-monotonous behavior of the field-induced gap with the minimum at about H_{sat} was demonstrated. The gap behavior was also described analytically by Fouet et al. [11]. Again, such a behavior can be understood taking into account the field-dependent staggered magnetization. The applied uniform magnetic field induces a local staggered field with the maximal transfer component. In high magnetic fields, before reaching the saturation the system cannot develop the transverse staggered magnetization anymore, changing the gap behavior (Fig. 4). This was ideed observed in Cu-PM with $H_{sat} = 48.5$ T, revealing excellent agreement

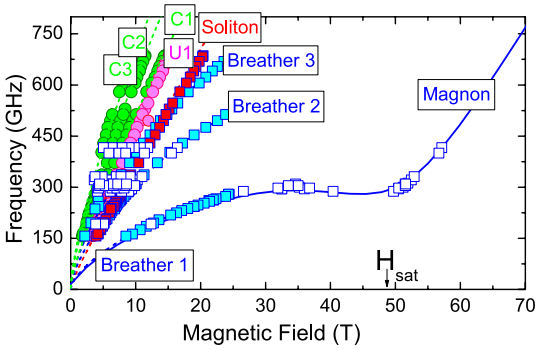

Fig. 6 Frequency-field diagram of magnetic excitations in Cu-PM in magnetic fields up to 63 T ($H \parallel c''$). The solid line corresponds to results of DMRG calculations. After Ref. [53]

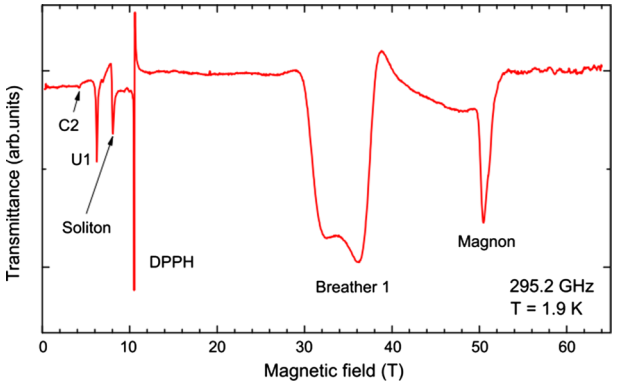

Fig. 7 Pulsed-field ESR spectrum in Cu-PM obtained at a frequency of 295.2 GHz. After Ref. [54]

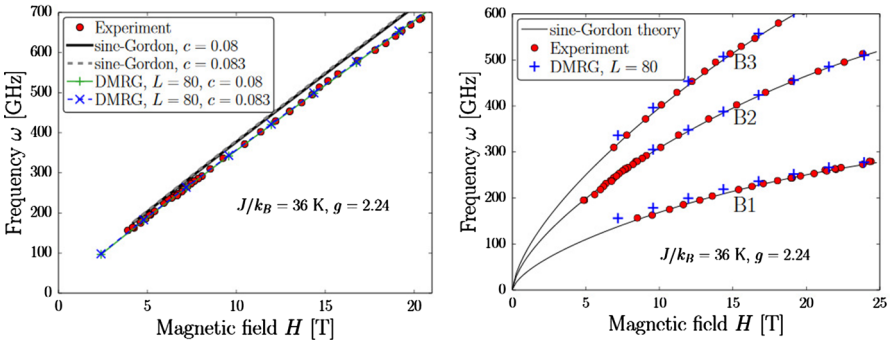

Fig. 8 The frequency-field diagram of the single-soliton resonance (left panel) and breathers (right panel), showing comparison between experimental data (symbols), DMRG (L=80), and field-theoretical calculation results. After Ref. [55]

with the results of DMRG calculations [53, 54]. An example of ESR spectrum in Cu-PM obtained at a frequency of 295.2 GHz is shown in Fig. 7.

Now I would like to comment on the recent progress in theoretical description of magnetic excitations in sine-Gordon spin chains. Based on numerical results obtained by the DMRG and exact diagonalization (ED), the spin dynamics in Cu-PM in applied magnetic fields was revisited [55]. Importantly, the calculations for momentum and frequency-resolved dynamical quantities give direct access to the intensity of the elementary excitations at both zero and finite temperature, allowing one to study the system beyond the low-energy description by the quantum-field sine-Gordon model. The theory provides a perfect description of the soliton-breather picture (Fig. 8). Interestingly, above $H_{\rm sat}$, the theory predicts the presence of the two-magnon continuum with a clearly visible lower-energy boundary (Fig. 9).

Apart from the soliton and breather modes, at least six more ESR modes were observed in Cu-PM (Fig. 5). Modes $C1-C3$ lie very close to the edges of the soliton-breather continua, and thus can be interpreted as transitions from the spin

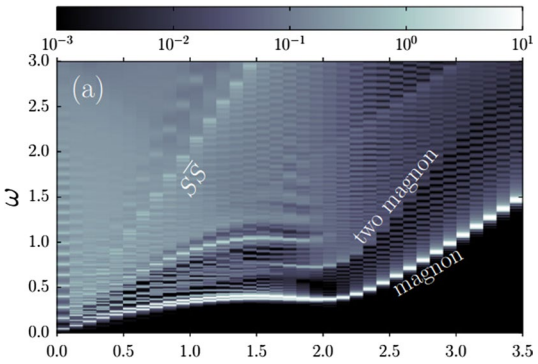

Fig. 9 The frequency-field plot of the absorption intensity at $T = 0$, obtained by DMRG-based Chebyshev expansions (order N=6000) at fixed fields $h_z \in [0,3.4]$ for a step increment of $\Delta h_z = 0.1$ and $L = 80$. After Ref. [55]

singlet ground state to the continuum edges. On the other hand, ESR revealed a number of magnetic excitations (modes $U1 - U3$), whose identification appears to be beyond the conventional sine-Gordon model. Similar to that, the presence of several additional excitations was revealed in another sine-Gordon spin-chain system, $KCuGaF_6$ (e.g., mode $U_1 - U_4$ in Fig. 10) [32]. The observation of these modes can be understood taking into account topological edge effects [56–58], resulting in emergence of so-called boundary bound-states, in addition to the spin states in the bulk. A boundary sine-Gordon field-theory approach to ESR in open spin-1/2 Heisenberg AF chains with an effective staggered field was developed [58]. Very good agreement between the theory and experimental observations in Cu-PM [23] and $KCuGaF_6$ [32] was demonstrated.

Solitons and breathers can be observed only at very low temperature, $T \ll \Delta/k_B$. At higher temperatures, the effect of alternating g-tensors and the staggered DM

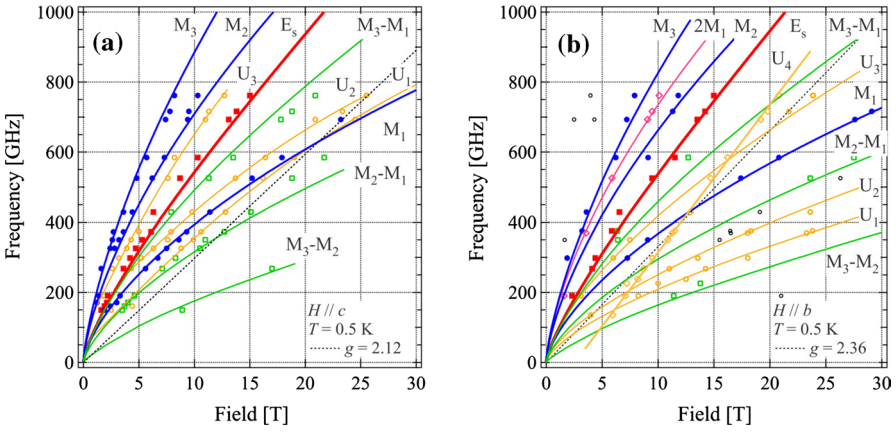

Fig. 10 Frequency-field diagrams of the ESR modes in $KCuGaF_6$ at $T = 0.5$ K for $H \parallel c$ (**a**) and $H \parallel b$ (**b**). Symbols denote the experimental results, and lines correspond to calculations based on the the sine-Gordon quantum-field theory approach. Modes E_s, M_1, M_2, M_3 correspond to soliton and breather excitations, respectively. Excitation modes M_3-M_1, M_2-M_1, M_3-M_2, correspond to transitions within excited states. After Ref. [32]

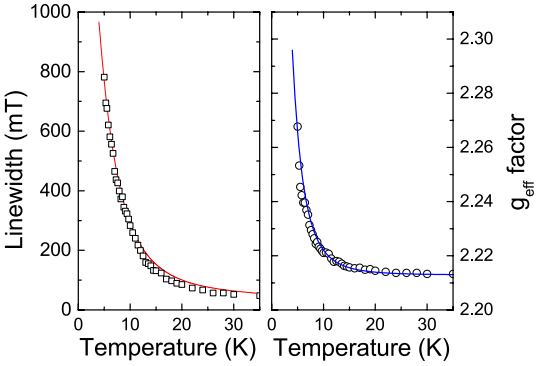

Fig. 11 Temperature dependences of ESR linewidth (left panel) and effective g factor (right panel) in Cu-PM at a frequency of 184 GHz ($H \parallel c''$). Symbols denote the experimental data, while solid lines correspond to the calculation results. After Ref. [24]

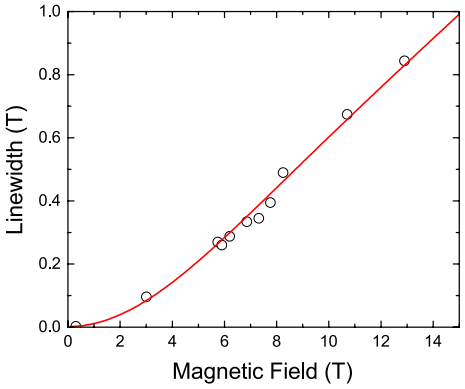

Fig. 12 Magnetic field dependence of ESR linewidth in Cu-PM measured at 10.3 K ($H \parallel c''$). Symbols denote the experimental data, while solid lines correspond to the calculation results. After Ref. [24]

interaction can be regarded as a perturbation, resulting in the nonlinear temperature- and field-dependent ESR frequency shift and the change in the linewidth [12, 13]. Importantly, the theory allows precise calculations of the ESR parameters.

First, such a behavior was revealed in Cu-benzoate [51, 59]. Later on, it was found [17] that terms $(H/T)^2$ and $(H/T)^3$ clearly dominate in the ESR linewidth and shift of the resonance field, respectively, being consistent with the theory for a spin-1/2 Heisenberg AF chain with the alternating g-tensor and/or DM interaction [12, 13]. In Fig. 11 the temperature dependences of the ESR linewidth and effective g-factor in Cu-PM at a frequency of 184 GHz are presented together with results of calculations [24]. Figure 12 shows the field dependence of the ESR linewidth in Cu-PM. In all cases excellent agreement with the theory [12, 13] was achieved. The obtained staggered field parameter c ($c = h/H$) is in excellent agreement with the value $c = 0.08$ found earlier from the analysis of the frequency-field dependence of ESR modes in Cu-PM in the soliton-breather regime [23].

Very recently, a field-induced gap has been observed in the organic compound $[Cu(pym)(H_2O)_4]SiF_6.H_2O$ (pym = pyrimidine), a chiral spin-1/2 chain system with fourfold staggered g-tensors and uniform DM interaction (Fig. 13) [60]. Although such an observation is reminiscent of that revealed in nonchiral alternating spin-1/2 chains, the gap behavior does not fit with the conventional sine-Gordon theory considered above. Possible explanation of such an effect was proposed by Furuya

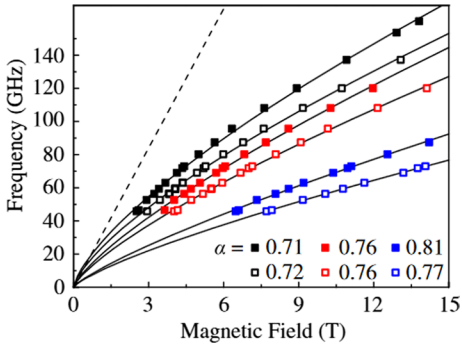

Fig. 13 The frequency-field diagram of magnetic excitations in $[Cu(pym)(H_2O)_4]SiF_6 \cdot H_2O$ at $T = 1.9$ K. Solid lines are fits to $f \propto H^{\alpha}$ with α values shown. Dashed line corresponds to the paramagnetic resonance with $g = 2$. After Ref. [60]

[61]. He argued that in analogy with that for the twofold staggered field, the fourfold screw fields breaks the one-site translational symmetry, giving rise to the excitation gap. However, the uniform DM interaction may cause additional nontrivial effects, such as field-induced changes in the spin-chain chirality, which can significantly affect the ESR excitation spectrum, as observed in the experiment.

In conclusion, I have reviewed recent experimental high-field ESR studies of the spin dynamics in spin-1/2 antiferromagnetic chain systems with the alternating g-tensors and staggered Dzyaloshinskii-Moriya interaction. The presence of a single soliton and four breathers was revealed in the excitation spectrum of Cu-PM, as predicted by the sine-Gordon quantum-field theory. Since high magnetic field tends to suppress quantum fluctuations, the excitation spectrum above the saturation field is determined by conventional magnons. Such a crossover from the soliton to magnon regime manifests itself in a nonmonotonic behavior of the field-induced gap, observed in Cu-benzoate and Cu-PM. The presence of extra spin states revealed in Cu-PM and $KCuGaF_6$ can be understood in terms of the boundary bound-state theory. These states are the consequence of the topological-edge effects, emerging due to the finite chain lengths. Another result of the symmetry-breaking effects in sine-Gordon chains is the specific temperature/field behavior of ESR parameters in the higher-temperature perturbative regime. Finally, I discussed the observation of the field-induced gap in $[Cu(pym)(H_2O)_4]SiF_6 \cdot H_2O$. The presence of the fourfold staggered g-tensor in this spin-1/2 chiral chain system makes the gap behavior very different from that observed previously in other spin-1/2 chains with the alternating g-tensors and staggered Dzyaloshinskii-Moriya interaction. The interpretation and quantitative analysis of all the presented experimental results are supported by calculations, revealing excellent agreement with the experiment.

Acknowledgements This work was supported by the Deutsche Forschungsgemeinschaft, through ZV 6/2-2 and SFB 1143, as well as by the HLD at HZDR, member of the European Magnetic Field Laboratory (EMFL). I thank Y. Ajiro, L. Bhaskaran, E. Čižmár, F. H. L. Essler, R. Feyerherm, S. C. Furuya, P. A. Goddard, A. Honecker, A. K. Kolezhuk, J. Krzystek, S. R. Manmana, F. Mila, H. Nojiri, M. Ozerov, M. Oshikawa, A. Ponomaryov, S. Süllow, A. C. Tiegel, A. U. B. Wolter-Giraud, and J. Wosnitza for their valuable contributions in the course of this work.

Funding Open Access funding enabled and organized by Projekt DEAL.

References

1. T. Giamarchi, *Quantum physics in one dimension*. International series of monographs on physics, vol. 121 (Oxford University Press, Oxford, 2004). https://www.worldcat.org/title/quantum-physics-in-one-dimension/oclc/488856710
2. T. Yamada, Prog. Theor. Phys. Jpn. **41**, 880 (1969)
3. G. Müller, H. Thomas, H. Beck, J.C. Bonner, Phys. Rev. B **24**, 1429 (1981)
4. M. Oshikawa, I. Affleck, Phys. Rev. Lett. **79**, 2883 (1997)
5. F.H.L. Essler, A.M. Tsvelik, Phys. Rev. B **57**, 10592 (1998)
6. F.H.L. Essler, Phys. Rev. B **59**, 14376 (1999)
7. I. Affleck and M. Oshikawa, Phys. Rev. B **60**, 1038 (1999); *ibid.* **62**, 9200 (2000)
8. F.H.L. Essler, A. Furusaki, T. Hikihara, Phys. Rev. B **68**, 064410 (2003)
9. J. Lou, S. Qin, C. Chen, Z. Su, L. Yu, Phys. Rev. B **65**, 064420 (2002)
10. J.Z. Zhao, X.Q. Wang, T. Xiang, Z.B. Su, L. Yu, Phys. Rev. Lett. **90**, 207204 (2003)
11. J.-B. Fouet, O. Tchernyshyov, F. Mila, Phys. Rev. B **70**, 174427 (2004)
12. M. Oshikawa, I. Affleck, Phys. Rev. Lett. **82**, 5136 (1999)
13. M. Oshikawa, I. Affleck, Phys. Rev. B **65**, 134410 (2002)
14. D.C. Dender, P.R. Hammar, D.H. Reich, C. Broholm, G. Aeppli, Phys. Rev. Lett. **79**, 1750 (1997)
15. H. Koizumi, K. Osaki, T. Watanabe, J. Phys. Soc. Jpn. **18**, 117 (1963)
16. D.C. Dender, D. Davidović, D.H. Reich, C. Broholm, K. Lefmann, G. Aeppli, Phys. Rev. B **53**, 2583 (1996)
17. T. Asano, H. Nojiri, Y. Inagaki, J.P. Boucher, T. Sakon, Y. Ajiro, M. Motokawa, Phys. Rev. Lett. **84**, 5880 (2000)
18. T. Asano, H. Nojiri, Y. Inagaki, T. Sakon, J.-P. Boucher, Y. Ajiro, M. Motokawa, Physica B: Cond. Matt. **329–333**, 1213–1214 (2003)
19. T. Asano, H. Nojiri, W. Higemoto, A. Koda, R. Kadono, Y. Ajiro, J. Phys. Soc. Jpn. **71**, 594 (2002)
20. H. Nojiri, Y. Ajiro, T. Asano, J.-P. Boucher, New J. Phys. **8**, 218 (2006)
21. R. Feyerherm, S. Abens, D. Günther, T. Ishida, M. Meißner, M. Meschke, T. Nogami, M. Steiner, J. Phys.: Condens. Matter **12**, 8495 (2000)
22. A.U.B. Wolter, H. Rakoto, M. Costes, A. Honecker, W. Brenig, A. Klümper, H.-H. Klauss, F.J. Litterst, R. Feyerherm, D. Jérome, S. Süllow, Phys. Rev. B **68**, 220406(R) (2003)
23. S.A. Zvyagin, A.K. Kolezhuk, J. Krzystek, R. Feyerherm, Phys. Rev. Lett. **93**, 027201 (2004)
24. S.A. Zvyagin, A.K. Kolezhuk, J. Krzystek, R. Feyerherm, Phys. Rev. Lett. **95**, 017207 (2005)
25. M. Kenzelmann, Y. Chen, C. Broholm, D.H. Reich, Y. Qiu, Phys. Rev. Lett. **93**, 017204 (2004)
26. M. Kenzelmann, C.D. Batista, Y. Chen, C. Broholm, D.H. Reich, S. Park, Y. Qiu, Phys. Rev. B **71**, 094411 (2005)
27. P. Fulde, B. Schmidt, P. Thalmeier, Europhys. Lett. **31**, 323 (1995)
28. M. Köppen, M. Lang, R. Helfrich, F. Steglich, P. Thalmeier, B. Schmidt, B. Wand, D. Pankert, H. Benner, H. Aoki, A. Ochiai, Phys. Rev. Lett. **82**, 4548 (1999)
29. M. Oshikawa, K. Ueda, H. Aoki, A. Ochiai, M. Kohgi, J. Phys. Soc. Jpn. **68**, 3181 (1999)
30. M. Kohgi, K. Iwasa, J.-M. Mignot, B. Fak, P. Gegenwart, M. Lang, A. Ochiai, H. Aoki, T. Suzuki, Phys. Rev. Lett. **86**, 2439 (2001)
31. R. Morisaki, T. Ono, H. Tanaka, H. Nojiri, J. Phys. Soc. Jpn. **76**, 063706 (2007)
32. I. Umegaki, H. Tanaka, T. Ono, H. Uekusa, H. Nojiri, Phys. Rev. B **79**, 184401 (2009)
33. I. Umegaki, H. Tanaka, T. Ono, M. Oshikawa, K. Sakai, Phys. Rev. B **85**, 144423 (2012)

34. I. Umegaki, H. Tanaka, N. Kurita, T. Ono, M. Laver, C. Niedermayer, C. Rüegg, S. Ohira-Kawamura, K. Nakajima, K. Kakurai, Phys. Rev. B **92**, 174412 (2015)
35. M. Herak, A. Zorko, D. Arčon, A. Potočnik, M. Klanjšek, J. van Tol, A. Ozarowski, H. Berger, Phys. Rev. B **84**, 184436 (2011)
36. K. Nawa, O. Janson, Z. Hiroi, Phys. Rev. B **96**, 104429 (2017)
37. M. Mola, S. Hill, P. Goy, M. Gross, Rev. Sci. Instrum. **71**, 186 (2000)
38. S.A. Zvyagin, J. Krzystek, P.H.M. van Loosdrecht, G. Dhalenne, A. Revcolevschi, Phys. B **346–347**, 1 (2004)
39. S.A. Zvyagin, M. Ozerov, E. Čižmár, D. Kamenskyi, S. Zherlitsyn, T. Herrmannsdörfer, J. Wosnitza, R. Wünsch, W. Seidel, Rev. Sci. Instrum. **80**, 073102 (2009)
40. A.-L. Barra, M. Goiran, R. Sessoli, Compt. Rend. Phys. **14**, 106 (2013)
41. K. Katsumata, J. Phys.: Condens. Matt. **12**, R589 (2000)
42. Y. Ajiro, J. Phys. Soc. Jpn **72** (Suppl. B), 12 (2003)
43. S.A. Zvyagin, Low Temp. Phys. **38**, 1032 (2012)
44. S.A. Zvyagin, J. Wosnitza, C.D. Batista, M. Tsukamoto, N. Kawashima, J. Krzystek, V.S. Zapf, M. Jaime, N.F. Oliveira, A. Paduan-Filho, Phys. Rev. Lett. **98**, 047205 (2007)
45. S.A. Zvyagin, D. Kamenskyi, M. Ozerov, J. Wosnitza, M. Ikeda, T. Fujita, M. Hagiwara, A.I. Smirnov, T.A. Soldatov, A.Y. Shapiro, J. Krzystek, R. Hu, H. Ryu, C. Petrovic, M.E. Zhitomirsky, Phys. Rev. Lett. **112**, 077206 (2014)
46. S.A. Zvyagin, D. Graf, T. Sakurai, S. Kimura, H. Nojiri, J. Wosnitza, H. Ohta, T. Ono, H. Tanaka, Nat. Comm. **10**, 1064 (2019)
47. Defined here as a 0.1–10 THz range of frequencies
48. F.H.L. Essler, A. Furusaki, T. Hikihara, Phys. Rev. B **68**, 064410 (2003)
49. H. Koizumi, K. Osaki, T. Watanabe, J. Phys. Soc. Jpn. **18**, 117 (1963)
50. J.C. Bonner, M.E. Fisher, Phys. Rev. **135**, A640 (1964)
51. M. Date, H. Yamazaki, M. Motokawa, S. Tazawa, Prog. Theor. Phys. Suppl. **46**, 194 (1970)
52. K. Oshima, K. Okuda, M. Date, J. Phys. Soc. Jpn. **15**, 757 (1978)
53. S.A. Zvyagin, E. Čižmár, M. Ozerov, J. Wosnitza, R. Feyerherm, S.R. Manmana, F. Mila, Phys. Rev. B **83**, 060409(R) (2011)
54. M. Ozerov, J. Wosnitza, E. Čižmár, R. Feyerherm, S.R. Manmana, F. Mila, S.A. Zvyagin, J. Low Temp. Phys. **170**, 268 (2013)
55. A.C. Tiegel, A. Honecker, T. Pruschke, A. Ponomaryov, S.A. Zvyagin, R. Feyerherm, S. Manmana, Phys. Rev. B **93**, 104411 (2011)
56. J. Lou, C. Chen, J. Zhao, X. Wang, T. Xiang, Z. Su, L. Yu, Phys. Rev. B **94**, 217207 (2005)
57. J. Lou, C. Chen, X. Wang, Phys. Rev. B **73**, 092407 (2006)
58. S.C. Furuya, M. Oshikawa, Phys. Rev. Lett. **109**, 247603 (2012)
59. K. Okuda, H. Hata, M. Date, J. Phys. Soc. Jpn. **33**, 1574 (1972)
60. J. Liu, S. Kittaka, R.D. Johnson, T. Lancaster, J. Singleton, T. Sakakibara, Y. Kohama, J. van Tol, A. Ardavan, B.H. Williams, S.J. Blundell, Z.E. Manson, J.L. Manson, P.A. Goddard, Phys. Rev. Lett. **122**, 057207 (2019)
61. S.C. Furuya, Phys. Rev. B **101**, 134425 (2020)